Global Journal of Researches in Engineering: A Mechanical and Mechanics Engineering
Volume 24 Issue 2 Version 1.0 Year 2024
Type: Double Blind Peer Reviewed International Research Journal
Publisher: Global Journals
Online ISSN: 2249-4596 & Print ISSN: 0975-5861

Thermal Vibration of Thick FGM Circular Cylindrical Shells by using Fully Homogeneous Equation and TSDT

By C. C. Hong
Hsiuping University of Science and Technology

Abstract- The third-order shear deformation theory (TSDT) effects on functionally graded material (FGM) thick circular cylindrical shells with entirely homogeneous equation under thermal vibration were investigated by using the generalized differential quadrature (GDQ) method. The nonlinear coefficient term of displacement field of TSDT was used in the equations of motion for thermal vibration of FGM thick circular cylindrical shells. Parametric effects of environment temperature and FGM power law index on the thermal stress and centre deflection of FGM thick circular cylindrical shells were investigated.

Keywords: *shear deformation theory, sinusoidal, stress, displacement, environment temperature, shear correction coefficient.*

GJRE-A Classification: *LCC: TA654, TA660.C9*

Strictly as per the compliance and regulations of:

Thermal Vibration of Thick FGM Circular Cylindrical Shells by using Fully Homogeneous Equation and TSDT

C. C. Hong

Abstract- **The third-order shear deformation theory (TSDT) effects on functionally graded material (FGM) thick circular cylindrical shells with entirely homogeneous equation under thermal vibration were investigated by using the generalized differential quadrature (GDQ) method. The nonlinear coefficient term of displacement field of TSDT was used in the equations of motion for thermal vibration of FGM thick circular cylindrical shells. Parametric effects of environment temperature and FGM power law index on the thermal stress and centre deflection of FGM thick circular cylindrical shells were investigated.**

Keywords: shear deformation theory, sinusoidal, stress, displacement, environment temperature, shear correction coefficient.

I. Introduction

Some studies of shear deformation effects in functionally graded material (FGM) shells were presented. In 2018, Cong et al. [1] used Reddy's third-order shear deformation theory (TSDT) for the nonlinear displacements to study the time response of displacements of double curves shallow shells. The effecting numerical solutions for honeycomb materials in geometrical parameters, material properties and damping loads were presented. In 2017, Sobhaniaragh et al. [2] used the TSDT for the displacements to study the buckling loads of FGM carbon nano-tube (CNT)-reinforced shells in an environment (room temperature 300K) without thermal strains, parametric effects on material properties and critical buckling loads were presented by using the generalized differential quadrature (GDQ) method. In 2017, Dung and Vuong [3] used an analytical method with TSDT to study the buckling of FGM shells in elastic foundation under thermal environment and external pressure. In 2016, Dai et al. [4] presented a 2000-2015 review focused on coupled mechanics, e.g. thermo-mechanical responses with the first-order shear deformation theory (FSDT) models, HSDT models in widely used TSDT to study the bending, buckling, free and forced vibrations of FGM cylindrical shells by using various theoretical, analytical and numerical methods. In 2016, Fantuzzi et al. [5] used the numerical GDQ methods to study the free vibration of FGM spherical and cylindrical shells, frequency solutions in FGM exponent number and thickness ratio were included. There were some numerical studies in the thick shells. In 2016, Kar and Panda [6] used the code of finite element method (FEM) and the TSDT displacements to get the numerical static bending results of deflections and stresses for the heated FGM spherical shells under thermal load and thermal environment. In 2015, Kurtaran [7] used the methods of GDQ and FSDT to get the numerical transient results of moderately thick laminated composite spherical and cylindrical shells. In 2012, Viola et al. [8] presented static analyses of FGM cylindrical shells under mechanical loading by using the GDQ method and a 2D unconstrained third-order shear deformation theory (UTSDT). The numerical solutions for stresses without thermal effect are obtained. In 2010, Sepiani et al. [9] used the FSDT formulation to get the numerical free vibration and buckling results for the FGM cylindrical shells without considering the thermal effect.

Many GDQ computational experiences in the composited FGM shells and plates were presented by including and considering the effects of thermal temperature of environment and heating loads. In 2017, Hong [10] presented the numerical thermal vibration results of FGM thick plates by considering the FSDT model and the varied shear correction factor effects. In 2017, Hong [11] presented the numerical thermal vibration and flutter results of a supersonic air flowed over FGM thick circular cylindrical shells by considering the FSDT model and the varied shear correction factor effects. In 2017, Hong [12] presented the numerical displacement and stresses results of FGM thin laminated magnetostrictive shells by considering with velocity feedback and suitable control gain values under thermal vibration. In 2016, Hong [13] presented the thermal vibration of Terfenol-D FGM circular cylindrical shells by considering the FSDT model and the constant modified shear correction factor effects. The computational GDQ solutions for the parametric effects of thickness of mounted Terfenol-D layer, control gain values, temperature of environment and power law index were investigated. In 2016, Hong [14] presented the transient response of Terfenol-D FGM circular cylindrical shells without considering the shear deformation effects. The computational GDQ solutions for the normal

Author: Department of Mechanical Engineering, Hsiuping University of Science and Technology, Taichung, Taiwan, ROC.
e-mail: cchong@mail.hust.edu.tw

direction displacement and thermal stress were obtained. In 2016, Hong [15] presented the investigation of rapid heating-induced vibration of Terfenol-D FGM circular cylindrical shells. The computational GDQ solutions for both the amplitudes of displacement and stress are increasing with rapid heating value. In 2015, Hong [16] presented the rapid heating-induced vibration of Terfenol-D FGM cylindrical shells with FSDT transverse shear effects. The computational GDQ solutions for thermal stresses and centre deflections in the parametric effects of magnetostrictive layer thickness, control gain values, temperature of environment, power law index of FGM shells and applied heat flux were obtained. In 2014, Hong [17] presented the thermal vibration and transient response of Terfenol-D FGM plates by considering the FSDT model and the varied modified shear correction factor effects. The computational GDQ solutions for the effect of different mechanical boundary conditions were investigated. In 2014, Hong [18] presented the rapid heating-induced vibration of Terfenol-D FGM circular cylindrical shells without considering the effects of shear deformation. The computational GDQ solutions for the displacement of Terfenol-D FGM shells versus the thickness of Terfenol-D is stable for all power law index values. It was interesting to investigate the thermal stresses and centre displacement of GDQ computation in this nonlinear TSDT vibration approach and the varied effects of shear correction coefficient of FGM circular cylindrical shells with four edges in simply supported boundary conditions. Two parametric effects of environment temperature and FGM power law index on the thermal stress and centre displacement of FGM circular cylindrical shells including the effect of varied shear correction coefficient were also investigated.

II. Formulation Procedure

For a two-material FGM circular cylindrical shell is shown in *Fig. 1* with thickness h_1 of inner layer FGM material 1 and thickness h_2 of outer layer FGM material 2, L is the axial length of FGM shells, h^* is the total thickness of FGM shells. The material properties of power-law function of FGM shells are considered with Young's modulus E_{fgm} of FGM in standard variation form of power law index R_n. The others are assumed in the simple average form [19]. The properties of individual constituent material of FGMs are functions of environment temperature T. The time-dependent of nonlinear displacements u, v and w of thick FGM circular cylindrical shells are assumed in the nonlinear coefficient c_1 term of TSDT equations can be referred to the displacement equations [20], with the parameters u_0 and v_0 are tangential displacements in the in-surface coordinates x and θ axes direction, respectively, w is transverse displacement in the out of surface coordinates z axis direction of the middle-plane of shells, ϕ_x and ϕ_θ are the shear rotations, R is the middle-surface radius of FGM shell, t is time. Coefficient for $c_1 = \frac{4}{3(h^*)^2}$ is used in the TSDT expression. Thus $c_1 = 0$ is used and became the FSDT mode.

For the normal direction stresses (σ_x and σ_θ) and the shear stresses ($\sigma_{x\theta}$, $\sigma_{\theta z}$ and σ_{xz}) in the thick FGM circular cylindrical shells under temperature difference ΔT for the kth layer can be referred to the constitutive equations in terms of stresses, stiffness and strains [21-22], with the parameters α_x and α_θ are the coefficients of thermal expansion, $\alpha_{x\theta}$ is the coefficient of thermal shear, $\overline{Q}_{ij}$ is the stiffness of FGM shells. ε_x, ε_θ and $\varepsilon_{x\theta}$ are in-plane strains, not negligible $\varepsilon_{\theta z}$ and ε_{xz} are shear strains.

A temperature difference ΔT between the FGM shell and curing area is given in functions of cylindrical coordinates x, θ and t. The heat conduction equation in simple form for the FGM shell in the cylindrical coordinates is used [13]. The dynamic equations of motion with TSDT for an FGM shell can be referred to the partial derivatives of external forces, thermal loads, mechanical loads and inertia terms [23], with the parameters $I_i = \sum_{k=1}^{N^*} \int_k^{k+1} \rho^{(k)} z^i dz$, ($i$= 0, 1, 2,…, 6), in which N^* is total number of layers, $\rho^{(k)}$ is the density of kth ply. $J_i = I_i - c_1 I_{i+2}$, $(i = 1,4)$, $K_2 = I_2 - 2c_1 I_4 + c_1^2 I_6$.

The Von Karman type of strain-displacement relations with $\frac{\partial v_0}{\partial z} = \frac{-v_0}{R}$, $\frac{\partial u_0}{\partial z} = \frac{-u_0}{R}$ and $\frac{\partial w}{\partial z} = \frac{\partial \phi_x}{\partial z} = \frac{\partial \phi_\theta}{\partial z} = 0$ are used to simplify the strain equations. Thus the dynamic equilibrium differential equations in the cylindrical coordinates with TSDT of FGM shells in terms of partial derivatives of displacements and shear rotations subjected to partial derivatives of thermal loads, mechanical loads (p_1, p_2, q) and inertia terms can be derived in matrix forms. By assuming that mid-plane strain terms $\frac{1}{2}(\frac{\partial w}{\partial x})^2$, $\frac{\partial w}{\partial x}\frac{\partial w}{R\partial \theta}$ and $\frac{1}{2}(\frac{\partial w}{R\partial \theta})^2$ are in constant values, the relative parameters are listed as follows,

$$(A_{i^s j^s}, B_{i^s j^s}, D_{i^s j^s}, E_{i^s j^s}, F_{i^s j^s}, H_{i^s j^s}) = \int_{\frac{-h^*}{2}}^{\frac{h^*}{2}} \overline{Q}_{i^s j^s}(1, z, z^2, z^3, z^4, z^6)dz, \ (i^s, j^s = 1,2,6),$$

$$(A_{i^* j^*}, B_{i^* j^*}, D_{i^* j^*}, E_{i^* j^*}, F_{i^* j^*}, H_{i^* j^*}) = \int_{\frac{-h^*}{2}}^{\frac{h^*}{2}} k_\alpha \overline{Q}_{i^* j^*}(1, z, z^2, z^3, z^4, z^5)dz, \ (i^*, j^* = 4,5), \quad (1)$$

in which p_1 and p_2 are external in-plane distributed forces in x and θ direction respectively. q is external pressure load, k_α is the shear correction coefficient, computed and varied values of k_α are usually functions of total thickness of shells, FGM power law index and environment temperature [24]. The $\overline{Q}_{i^s j^s}$ and $\overline{Q}_{i^* j^*}$ for FGM thick circular cylindrical shells with z/R terms cannot be neglected are used in the simple forms in 2010 by Sepiani et al. [9] [24].

The time sinusoidal displacements and shear rotations are varied with $\sin(\omega_{mn} t)$ can be referred [13]. The time sinusoidal temperature difference ΔT of thermal vibration is assumed in the following simple equation varied with $\sin(\gamma t)$,

$$\Delta T = \frac{z}{h^*} \bar{T}_1 \sin(\pi x/L) \sin(\pi\theta/R) \sin(\gamma t), \quad (2)$$

where ω_{mn} is the natural frequency in mode shape subscript numbers m and n of the shells, γ is the frequency of applied heat flux, $\bar{T}_1$ is the amplitude of applied temperature.

The GDQ numerical method is presented and referred [17][25-27]. The boundary conditions in dynamic GDQ discrete equations approach are to be considered for four sides simply supported, not symmetric, orthotropic of laminated FGM thick circular cylindrical shells and assumed that $A_{16} = A_{26} = 0$, $B_{16} = B_{26} = 0$, $D_{16} = D_{26} = 0$, $E_{16} = E_{26} = 0$, $F_{16} = F_{26} = 0$, $H_{16} = H_{26} = 0$, $A_{45} = D_{45} = F_{45} = 0$ under sinusoidal temperature loading. For a typical grid point (i, j), the dynamic GDQ discrete equations can be rewritten into the matrix form as follows,

$$[A]\{W^*\} = \{B\}, \quad (3)$$

where $[A]$ is a dimension of N^{**} by N^{**} coefficient matrix ($N^{**} = (N-2)\times(M-2)\times 5$), $\{W^*\}$ is a N^{**} th-order unknown column vector and $\{B\}$ is a N^{**} th-order row external loads vector.

III. Numerical Results

The FGM material 1 is SUS304, the FGM material 2 is Si_3N_4 used for the numerical computations under four sides simply supported. The frequency γ of applied heat flux for the thermal loads is given in the heat conduction equation can be reduced and simplified [13]. It is needed to get the calculation values of ω_{mn} under $p_1 = p_2 = 0$ and $q = 0$ for the free vibration. It is reasonable to assumed that u_0, v_0, w, ϕ_x and ϕ_θ are expressed in the referred time sinusoidal form of free vibration and expressed in the referred entirely homogeneous matrix equation [29] with varied parameters $m\pi/L$ and $n\pi/R$. The determinant of the coefficient matrix in the entirely homogeneous equation vanishes for obtaining non-trivial solution of amplitudes, thus the ω_{mn} and γ can be found.

The non-dimensional frequency $\Omega = (\omega_{11} L^2/h^*)\sqrt{\rho_1/E_1}$ and $f^* = 4\pi\omega_{11} R\sqrt{I_2/A_{11}}$ for SUS304/Si_3N_4 thick circular cylindrical shells with entirely homogeneous equation and TSDT under free vibration are compared with published literature as shown in *Table 1,* in which ω_{11} is the fundamental first natural frequency $m = n = 1$, ρ_1 is the density of FGM material 1. The present value of Ω =1.906986 on c_1 =0.925925/mm^2, L/h^* =10, h^* =1.2mm, T=700K, R_n =1 is in close to the value of Ω =1.65127 with the material variation type A, three layers thickness ratio 1-8-1, the L directional radius of curvature is ∞, L/h^* =10, R_n =1 for the FGM sandwich shell presented by Chen et al. [28]. The present value of f^* =5.041756 at L/h^* =10, h^* =2mm, T=300K, R_n =0.5 is in close to the value of f^* =5.10 on n =9 with silicon nitride–nickel under classical shell theory (CST), no external pressure (*Ke*= 0) by Sepiani et al. [9].

The following coordinates x_i and θ_j for the grid points numbers N and M of FGM thick circular cylindrical shells are used to study the GDQ results,

$$x_i = 0.5[1 - \cos\left(\frac{i-1}{N-1}\pi\right)]L, \ i = 1,2,\ldots,N,$$

$$\theta_j = 0.5[1 - \cos\left(\frac{j-1}{M-1}\pi\right)]R, \ j = 1,2,\ldots,M. \quad (4)$$

The convergence of centre deflection $w(L/2, 2\pi/2)$ (mm) in the thermal vibration under c_1 =0.925925 and c_1 =0 for FGM thick circular cylindrical shells L/h^* = 10 with applied heat flux γ =0.2618004/s and L/h^* =5 with γ =0.2618019/s, respectively at t = 6s, $L/R = 1$, h^* =1.2mm, $h_1 = h_2$ =0.6mm, T=100K,

$\bar{T}_1$ =100K are presented in *Table 2.* Considering the varied effects of k_α and ω_{11} for three values of R_n, in the nonlinear case of c_1 =0.925925/mm^2: (a) for value of R_n =0.5, k_α =0.111874 and ω_{11} =0.0001156/s are obtained. (b) for value of R_n =1, k_α =0.149001 and ω_{11} =0.0001151/s are obtained. (c) for value of R_n =2, k_α =0.231364 and ω_{11} =0.000114/s are obtained. In the linear case of c_1 =0/mm^2: (d) for value of R_n =0.5, k_α =0.111874 and ω_{11} =0.001000/s are obtained. (e) for value of R_n =1, k_α =0.149001 and ω_{11} =0.001000/s are obtained. (f) for value of R_n =2, k_α =0.231364 and ω_{11} =0.001000/s are obtained. The error accuracy is 0.000011 for the $w(L/2,2\pi/2)$ in R_n =0.5 and L/h^* = 10. The $N\times M$ =13×13 grid points can be used in the following GDQ computations of time responses for deflection and stress.

The $w(L/2,2\pi/2)$ (mm) for the thermal vibration of FGM thick circular cylindrical shells are calculated with varied γ and ω_{11}. The γ values are decreasing from γ =15.707960/s at t =0.1s to γ =0.523601/s at t =3.0s used for L/h^* =5, from γ =15.707963/s at t =0.1s to γ =0.523599/s at t =3.0s used for L/h^* =10. *Fig. 2* shows the response values of $w(L/2,2\pi/2)$ (mm) versus time t under c_1 =0.925925/mm^2 and c_1 =0 for thick L/h^* =5 and 10, respectively, $L/R=1$, $R_n=1$, k_α =0.120708, T=600K, $\bar{T}_1$ =100K during t =0.1s-3.0s. The maximum absolute value of $w(L/2,2\pi/2)$ is 33.955818mm occurs at t =0.1s for thick L/h^* =5 with c_1 =0.925925/mm^2 and γ =15.707963/s. The maximum absolute value of $w(L/2,2\pi/2)$ is 267.064789mm occurs at t = 0.1s for thick L/h^* =10 with c_1 =0/mm^2 and γ =15.707963/s.

Usually the normal direction stress σ_x and shear stress $\sigma_{x\theta}$ are three-dimensional components and in functions of x, θ and z for the thermal vibration of nonlinear TSDT FGM circular cylindrical shells as shown in *Fig. 3.* Typically their values vary through the thickness direction of circular cylindrical shells. *Fig. 3a* shows the normal direction stress σ_x(GPa) versus z/h^* and *Fig. 3b* shows the shear stress $\sigma_{x\theta}$ (GPa) versus z/h^* on centre position $x=L/2$ and $\theta=2\pi/2$ of FGM circular cylindrical shells, respectively at t =3.0s for thick a/h^* =10 with c_1 =0.925925/mm^2 and R_n =1. The value 1.702E-03GPa of σ_x on z =-0.5 h^* is found in the greater value than the value 1.955E-04GPa of $\sigma_{x\theta}$ on z =0.5 h^*, thus the σ_x can be treated as the dominated stress. *Figs. 3c-3d* show the time responses of the σ_x(GPa) on centre position of inner surface z =-0.5 h^* for R_n =1, thick L/h^* =5 and 10 with c_1 =0.925925/mm^2, respectively. The maximum value of σ_x is 2.005E-03GPa occurs at t =0.1s in the periods t =0.1s-3s for thick L/h^* =5.

In *Fig. 4* shows the response values of $w(L/2,2\pi/2)$ (mm) versus T in 100K, 600K and 1000K with R_n values from 0.1 to 10 for thick L/h^* =5 and 10, respectively under c_1 =0.925925/mm^2, $\bar{T}_1$ =100K, γ and k_α at t =0.1s. *Fig. 4a* shows the curves of $w(L/2,2\pi/2)$ vs. T and R_n for the L/h^* =5 case, the maximum absolute value of $w(L/2,2\pi/2)$ is 49.057815mm occurs in T=1000K for R_n = 2. The $w(L/2,2\pi/2)$ absolute values are all decreasing versus T from T=600K to T=1000K, for R_n =5 only, it can withstand for higher T=1000K. *Fig. 4b* shows the curves of $w(L/2,2\pi/2)$ vs. T and R_n for the L/h^* =10 case, they are almost located in the same curves for all value of R_n. The maximum value of $w(L/2,2\pi/2)$ is 7.039238mm occurs in T=1000K for all value of R_n. The $w(L/2,2\pi/2)$ values are all increasing versus T for all value of R_n, the amplitude $w(L/2,2\pi/2)$ of the L/h^* =10 cannot withstand for higher T=1000K.

In *Fig. 5* shows the σ_x(GPa) on centre position of inner surface z =-0.5 h^* versus T and all different values R_n for the thermal vibration of thick L/h^* =5 and 10 cases. *Fig. 5a* shows the curves of σ_x vs. T and R_n for the L/h^* =5 case, the values of σ_x versus T are all increasing from T=100K to T=600K and then all decreasing from T=600K to T=1000K for all value of R_n. The maximum value of σ_x is 0.002018GPa occurs on T=600K for R_n =2. The stress σ_x of the L/h^* =5 can withstand for higher T=1000K. *Fig. 5b* shows the curves of σ_x vs. T and R_n for the L/h^* =10 case, they are all located in the same curves for all value of R_n, the values of σ_x versus T are all increasing from T=100K to T=600K and then all decreasing from T=600K to T=1000K for all value of R_n. The maximum value of σ_x is 0.001745GPa occurs on T=600K. The stress σ_x of the L/h^* =10 can withstand for higher T=1000K.

IV. Conclusions

The GDQ solutions could be calculated and investigated for the deflections and stresses in the thermal vibration of FGM thick circular cylindrical shells by considering the varied effects of shear correction coefficient and nonlinear coefficient c_1 term of TSDT. The novel contribution of the GDQ stress and deflection solutions work is to investigate the effects of over estimation and under estimation of nonlinear coefficient term of TSDT in the thermal vibration of FGM circular shells. The natural frequency and parameter results of frequency including the entirely element effect in the homogeneous equation are also investigated and used to calculate the corresponding results in dynamic

convergence, vibration response of deflections and stresses.

References Références Referencias

1. Cong, P.H., Khanh, N.D., Khoa, N.D., Duc, N.D., 2018. New approach to investigate nonlinear dynamic response of sandwich auxetic double curves shallow shells using TSDT. Composite Structures 185, 455–465.
2. Sobhaniaragh, B., Nejati, M., Mansur, W.J., 2017. Buckling modelling of ring and stringer stiffened cylindrical shells aggregated by graded CNTs. Composites Part B 124, 120–133.
3. Dung, D.V., Vuong, P.M., 2016. Analytical investigation on buckling and postbuckling of FGM toroidal shell segment surrounded by elastic foundation in thermal environment and under external pressure using TSDT. Acta Mechanica 228, 3511–3531.
4. Dai, H.L., Rao, Y.N., Dai, T., 2016. A review of recent researches on FGM cylindrical structures under coupled physical interactions 2000–2015. Composite Structures 152, 199–225.
5. Fantuzzi, N., Brischetto, S., Tornabene, F., Viola, E., 2016. 2D and 3D shell models for the free vibration investigation of functionally graded cylindrical and spherical panels. Composite Structures 154, 573–590.
6. Kar, V.R., Panda, S.K., 2016. Nonlinear thermomechanical deformation behaviour of P-FGM shallow spherical shell panel. Chinese Journal of Aeronautics 29, 173–183.
7. Kurtaran, H., 2015. Geometrically nonlinear transient analysis of moderately thick laminated composite shallow shells with generalized differential quadrature method. Composite Structures 125, 605–614.
8. Viola, E., Rossetti, L., Fantuzzi, N., 2012. Numerical investigation of functionally graded cylindrical shells and panels using the generalized unconstrained third order theory coupled with the stress recovery. Composite Structures 94, 3736–3758.
9. Sepiani, H.A., Rastgoo, A., Ebrahimi, F., Arani, A.G., 2010. Vibration and buckling analysis of two-layered functionally graded cylindrical shell considering the effects of transverse shear and rotary inertia. Materials and Design 31, 1063–1069.
10. Hong, C.C., 2017. Varied effects of shear correction on thermal vibration of functionally graded material plates. Journal of Mechanical Engineering and Biomechanics 2, 1–7.
11. Hong, C.C., 2017. Effects of varied shear correction on the thermal vibration of functionally-graded material shells in an unsteady supersonic flow. Aerospace 4, 1–15.
12. Hong, C.C., 2017. The GDQ method of thermal vibration laminated shell with actuating magnetostrictive layers. International Journal of Engineering and Technology Innovation 7, 188–200.
13. Hong, C.C., 2016. Thermal vibration of magnetostrictive functionally graded material shells with the transverse shear deformation effects. Applications and Applied Mathematics: An International Journal 11, 127–151.
14. Hong, C.C. 2016. Transient response of functionally graded material circular cylindrical shells with magnetostrictive layer. Journal of Mechanics 32, 473–478.
15. Hong, C.C., 2016. Rapid heating-induced vibration of composite magnetostrictive shells. Mechanics of Advanced Materials and Structures 23, 415–422.
16. Hong, C.C., 2015. Rapid heating induced vibration of magnetostrictive functionally graded material cylindrical shells with transverse shear effects. Universal Journal of Structural Analysis 3, 35–47.
17. Hong, C.C., 2014. Thermal vibration and transient response of magnetostrictive functionally graded material plates. European Journal of Mechanics - A/Solids 43, 78–88.
18. Hong, C.C., 2014. Rapid heating induced vibration of circular cylindrical shells with magnetostrictive functionally graded material. Archives of Civil and Mechanical Engineering 14, 710–720.
19. Chi, S.H., Chung, Y.L., 2006. Mechanical behavior of functionally graded material plates under transverse load, Part I: Analysis. International Journal of Solids and Structures 43, 3657–3674.
20. Lee, S.J., Reddy, J.N., Rostam-Abadi, F., 2004. Transient analysis of laminated composite plates with embedded smart-material layers. Finite Elements in Analysis and Design 40, 463–483.
21. Lee, S.J., Reddy, J.N., 2005. Non-linear response of laminated composite plates under thermomechanical loading. Int. J. of Non-lin. Mech. 40, 971–985.
22. Whitney, J.M., 1987. Structural analysis of laminated anisotropic plates. Lancaster: Pennsylvania, USA, Technomic Publishing Company, Inc.
23. Reddy, J.N., 2002. Energy principles and variational methods in applied mechanics. Wiley, New York.
24. Hong, C.C., 2014. Thermal vibration of magnetostrictive functionally graded material shells by considering the varied effects of shear correction coefficient. International Journal of Mechanical Sciences 85, 20–29.
25. Hong, C.C., 2007. Thermal vibration of magnetostrictive material in laminated plates by the GDQ method. The Open Mech. J. 1, 29–37.
26. Bert, C.W., Jang, S.K., Striz, A.G., 1989. Nonlinear bending analysis of orthotropic rectangular plates by the method of differential quadrature. Computational Mechanics 5, 217–226.

27. Shu, C., Du, H., 1997. Implementation of clamped and simply supported boundary conditions in the GDQ free vibration analyses of beams and plates. International Journal of Solids and Structures 34, 819–835.
28. Chen, H., Wang, A., Hao, Y., Zhang, W., 2017. Free vibration of FGM sandwich doubly-curved shallow shell based on a new shear deformation theory with stretching effects. Composite Structures 179, 50–60.
29. Hong, C.C., 2019. GDQ computation for thermal vibration of thick FGM plates by using fully homogeneous equation and TSDT. Thin-Walled Structures 135, 78–88.

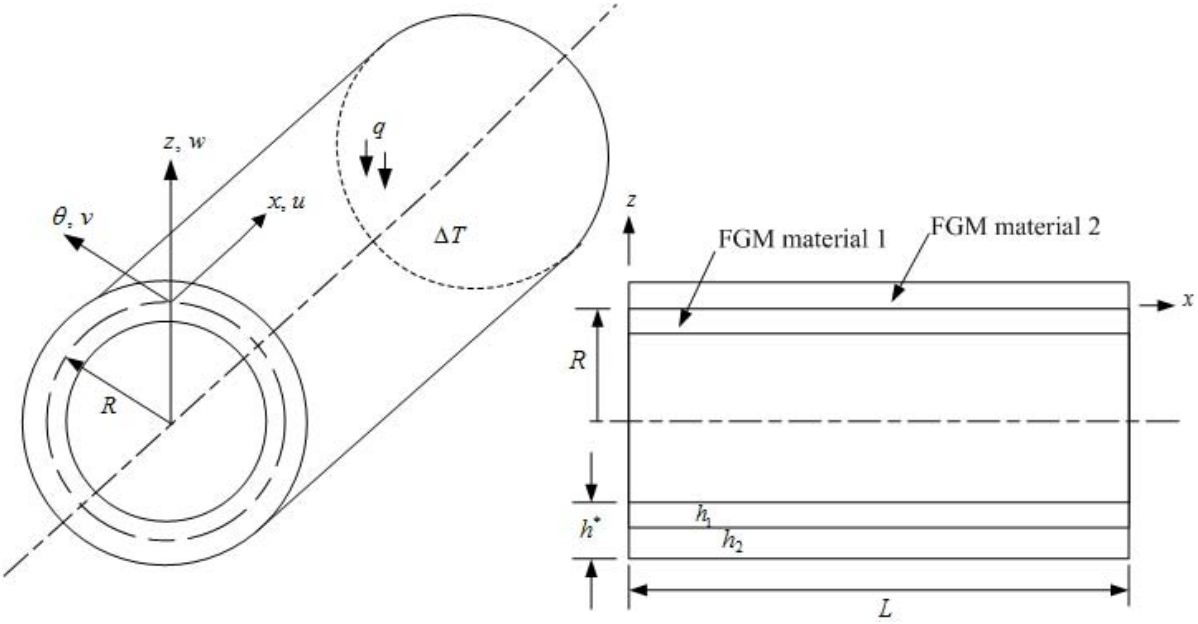

Fig. 1: Two-material FGM circular cylindrical shell

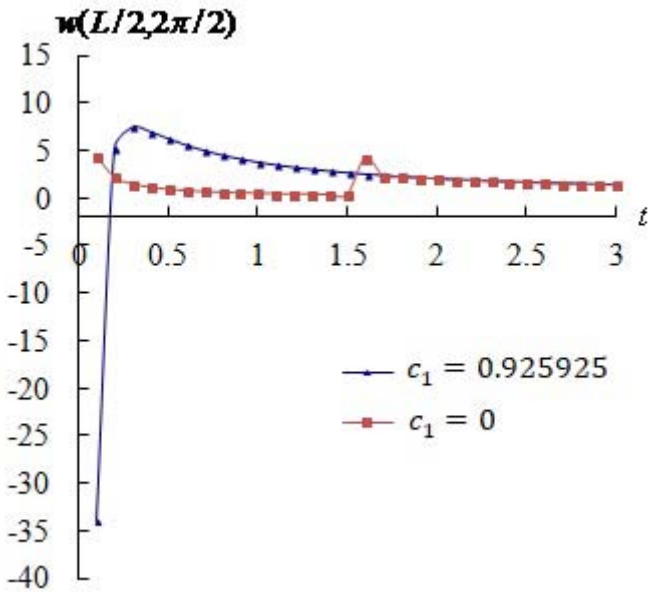

Fig. 2a: $w(L/2,2\pi/2)$ versus t for $L/h^* = 5$

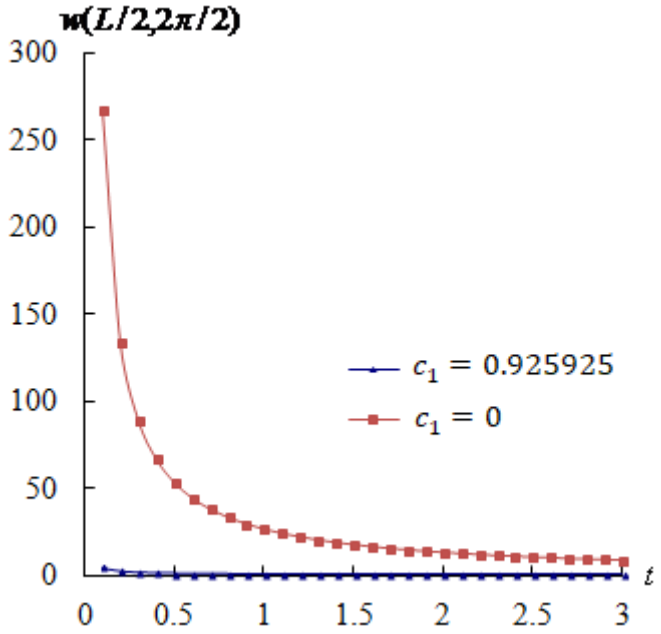

Fig. 2b: $w(L/2,2\pi/2)$ versus t for $L/h^* = 10$

Fig. 2: $w(L/2,2\pi/2)$ (mm) versus t (s) for $L/h^* = 5$ and 10

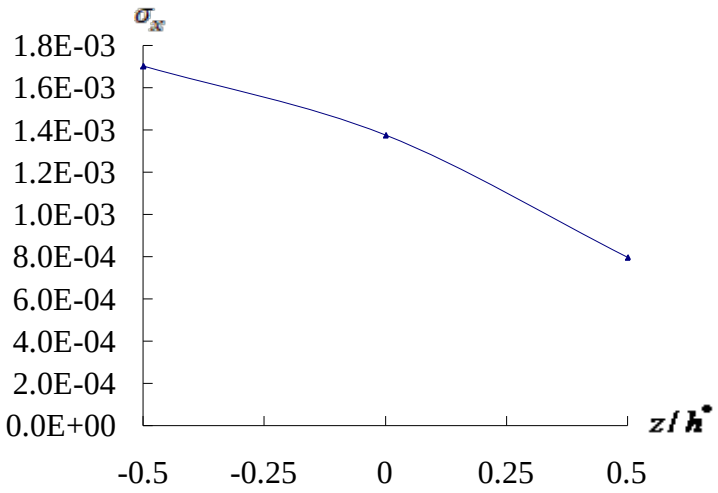

Fig. 3a: σ_x versus z/h^* for $L/h^* = 10$

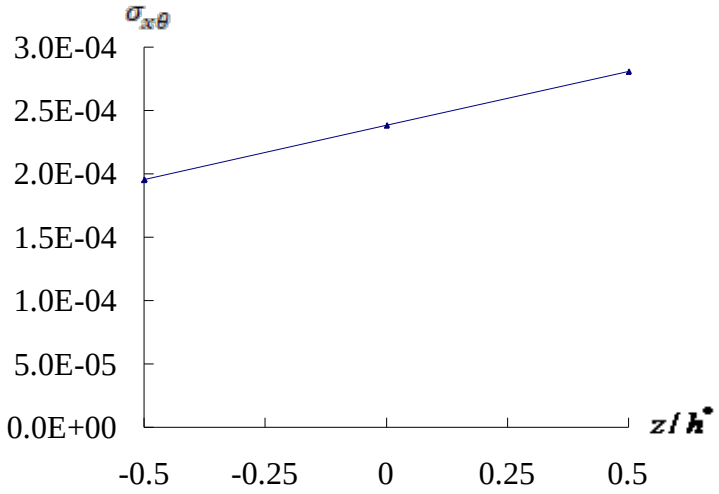

Fig. 3b: $\sigma_{x\theta}$ versus z/h^* for $L/h^*=10$

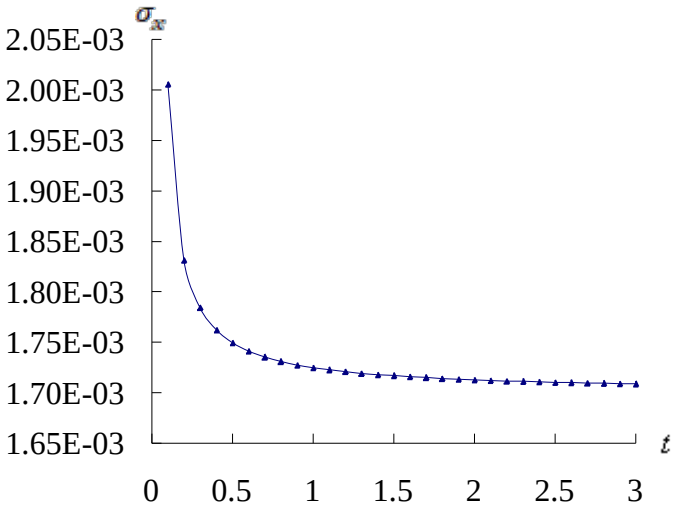

Fig. 3c: σ_x versus t for $L/h^*=5$

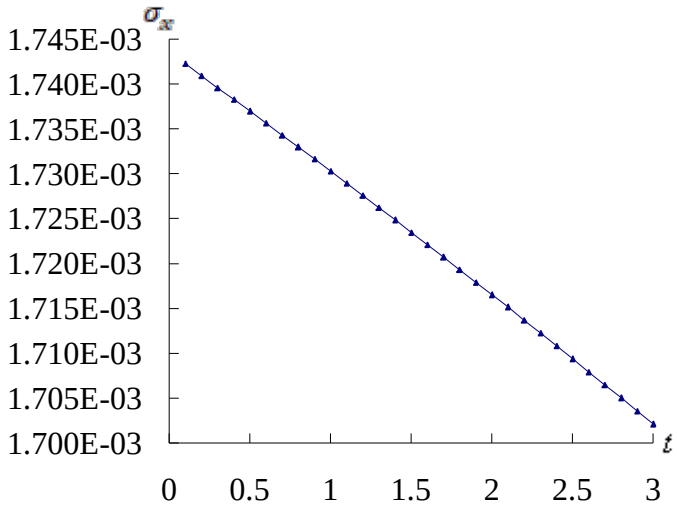

Fig. 3d: σ_x versus t for $L/h^*=10$

Fig. 3: Stresses (GPa) versus z/h^* and t (s) for $L/h^*=5$ and 10

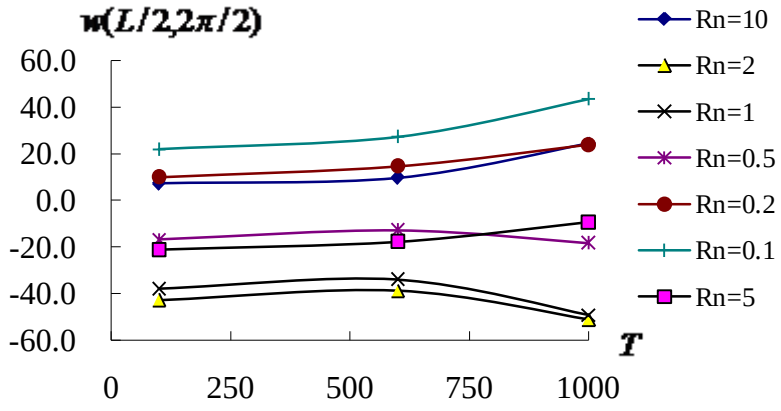

Fig. 4a: $w(L/2,2\pi/2)$ versus *T* for $L/h^*=5$ with R_n from 0.1 to 10

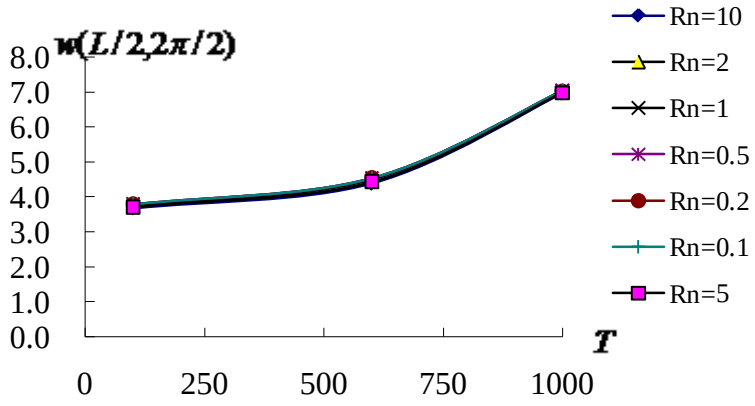

Fig. 4b: $w(L/2,2\pi/2)$ versus *T* for $L/h^*=10$ with R_n from 0.1 to 10

Fig. 4: $w(L/2,2\pi/2)$ (mm) versus *T* (K) for $L/h^*=5$ and 10

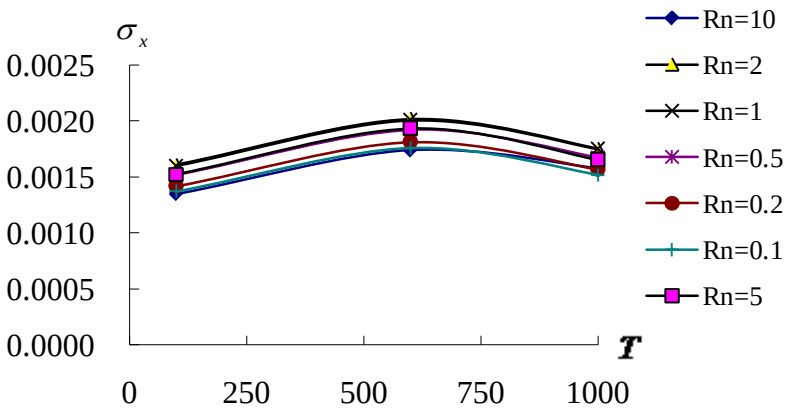

Fig. 5a: σ_x versus T for $L/h^*=5$

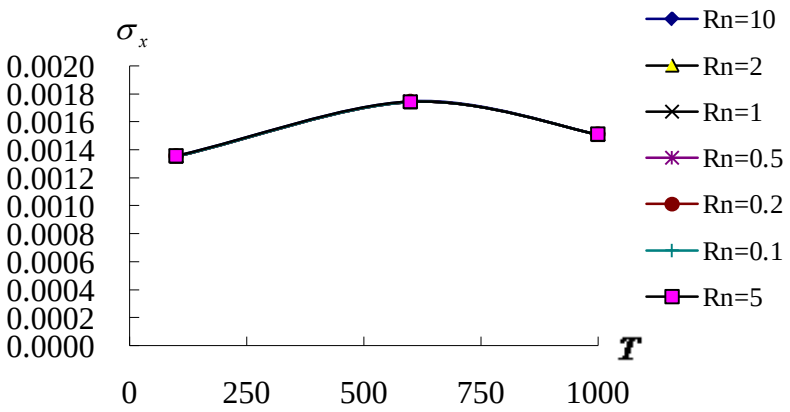

Fig. 5b: σ_x versus T for $L/h^* = 10$

Fig. 5: σ_x(GPa) versus T (K) for $L/h^* = 5$ and 10

Table 1: Compared values of Ω and f^* for SUS304/Si_3N_4

c_1 (1/mm²)	h^* (mm)	Ω		f^*	
		Present method, T=700K $R_n = 1$	Chen et al. 2017, type A, 1-8-1 $R_n = 1$ [28]	Present method, T=300K, $R_n = 0.5$	Sepiani et al. 2010, silicon nitride–nickel [9]
0.925925	1.2	1.906986	1.65127	0.517127	-
0.333333	2	11.14739	-	5.041756	5.10
0.000033	200	17704.31	-	800796.6	-
0.000014	300	3771.748	-	253980.0	-

Table 2: Dynamic convergence of the nonlinear TSDT FGM thick circular cylindrical shells

c_1 (1/mm²)	L/h^*	GDQ grids	$w(L/2, 2\pi/2)$ (mm) at $t = 6s$		
		$N \times M$	$R_n = 0.5$	$R_n = 1$	$R_n = 2$
0.925925	10	7 × 7	5.093878	5.113268	5.162740
		9 × 9	5.086901	5.107157	5.157094
		11 × 11	5.086960	5.107170	5.157115
		13 × 13	5.086899	5.107180	5.157098
	5	7 × 7	0.591193	0.595686	0.615068
		9 × 9	0.589491	0.594395	0.614112
		11 × 11	0.589487	0.594404	0.614114
		13 × 13	0.589495	0.594400	0.614107
0	10	7 × 7	23.807663	20.502832	21.591730
		9 × 9	3.210114	3.212350	3.193146
		11 × 11	3.216680	3.219491	3.210730
		13 × 13	3.213940	3.215927	3.197326
	5	7 × 7	0.524448	0.621863	0.832298
		9 × 9	0.505710	0.599383	0.798741
		11 × 11	0.505719	0.599400	0.798779
		13 × 13	0.505719	0.599401	0.798781